Research Article

Diffusion-weighted MRI for diagnosis and differential diagnosis of lymphatic malformation in paediatric patients

Alexander Sauer[1], Verena Müller[2], Thomas Pabst[1], Henning Neubauer[1 *]
[1] Department of Diagnostic and Interventional Radiology, [2]Department of Paediatrics
University Hospital Wuerzburg, 97080 Wuerzburg, Germany

***Corresponding author**: Henning Neubauer, MD, MBA. Department of Radiology, University Hospital Wuerzburg, Oberduerrbacher Str. 6, 97080 Wuerzburg, Germany. Phone: 0049-931-201-34715; Email: neubauer_h@ukw.de, inu75@web.de

Citation: Alexander Sauer, et al. Diffusion-weighted MRI for diagnosis and differential diagnosis of lymphatic malformation in paediatric patients. *Cancer Research Frontiers*. 2016 May; 2(2): 300-310. doi: 10.17980/2016.300

Copyright: @ 2016 Alexander Sauer, et al. This is an open-access article distributed under the terms of the Creative Commons Attribution License, which permits unrestricted use, distribution, and reproduction in any medium, provided the original author and source are credited.

Competing Interests: The authors declare no competing financial interests.
Received Mar 8, 2016; Revised May 13, 2016; Accepted May 27, 2016. Published June 7, 2016

Abstract

Background: Diffusion-weighted imaging (DWI) is a useful technique for characterisation and differentiation of various tumour entities. We studied the diagnostic value of DWI in children with lymphatic malformation (LM) and tumours mimicking LM.

Patients and Methods: Twenty consecutive patients (median 8 years, range 36 days to 17 years, females n=6) with histologically proven LM (n=16) or histologically confirmed masses mimicking LM on ultrasonography (n=4) underwent routine MRI at 1.5 Tesla including DWI. We retrospectively analysed imaging features on ultrasonography and MRI with particular emphasis on imaging artefacts secondary to intralesional haemorrhage.

Results: All tumour manifestations were detectable on DWI. Mean apparent diffusion coefficient (ADC, unit: x 10^{-3} mm^2/s) was high with 2.6 ± 0.3 in non-complicated LM (n=12). Partial signal loss, fluid-fluid levels and low signal on the ADC map was observed in the presence of intralesional haemorrhage, which coincided with signal loss in gradient-echo T2*w and with hyperechogenic signal on ultrasonography. Two patients with a large ranula and an infected branchiogenic cyst showed ADC values similar to LM, while DWI suggested a highly cellular mass in another patient eventually confirmed with Hodgkin disease.

Conclusion: DWI is a fast, non-invasive and useful supplement to conventional MRI for the differential diagnosis of complex cystic masses or in cases of tumours of uncertain dignity. Non-complicated lympangioma, haemorrhagic lymphatic malformation and solid tumours each show characteristic signal patterns on DWI.

Keywords: MRI; diffusion-weighted; lymphatic malformation; differential diagnosis; paediatric

Introduction

Lymphatic malformations (LM), or lymphangiomas, are rare congenital vascular tumours characterised by abnormal expansion of lymphatic spaces [1]. This entity is most common in the head and neck region, but may be encountered in many other anatomical regions, including axilla, mediastinum, abdominal wall, viscera, mesentery and the lower extremity [1-3]. As LMs are biologically benign, cosmetic issues constitute the primary concern in many patients. Yet, depending on location and size of the tumour,

functional impairment, or even life-threatening complications, such as air-way obstruction [2] or small-bowel volvulus [4], may result. While spontaneous regression or resolution has been observed in 2% to 40% of patients [5], the majority of patients needs surgical or interventional therapy at some point [6]. Haemorrhagic transformation, or infection, can trigger acute clinical exacerbation in previously asymptomatic patients, including progressive swelling and pain [7]. Haemorrhage has recently been observed in fetal LM [8]. Ultrasonography usually serves as the first line imaging modality, but MRI offers better visualisation of tumour extent and possibly accompanying pathologies and provides a wider range of diagnostic tools for differential diagnosis and preoperative planning [9]. Diffusion-weighted MR imaging (DWI) utilises the varying degree of restriction in Brownian diffusion in vivo to characterise biological tissues, mainly in terms of cellularity [10]. Added diagnostic value of DWI has been reported for paediatric musculoskeletal tumours [11] and for differential diagnosis of orbital tumours, including LM, in children [12]. In fact, one of the first reports on the utility of DWI in characterising paediatric tumours featured the case of a young girl with acute abdominal symptoms in which DWI provided crucial information for differentiation between suspected lymphoma and atypical abdominal lymphangiomatosis [13]. Diagnostic difficulties and pitfalls occasionally arise in paediatric LM patients with unusual presentation in terms of clinical symptoms, tumour location and imaging features. We therefore used diffusion-weighted MRI to study the imaging characteristics of LM and lesions mimicking LM on ultrasonography.

Patients and methods

We retrospectively identified all patients younger than 18 years of age examined at our institution between 2010 and 2014 with histologically confirmed LM (n=16) and histologically confirmed masses mimicking LM (n=4) at initial presentation. Three more patients with suspected LM, who had clinical and imaging follow-up, but no biopsy or resection, were excluded from this study.

All study work was conducted in accordance with the Helsinki Declaration. Informed written consent was obtained from the legal guardians of all patients for all diagnostic and therapeutic procedures. A waiver was granted by our Institutional Review Board for the retrospective analysis of anonymised routine imaging data, as presented in this study.

Our study group comprises 20 consecutive patients with a median age of 8 years (range 36 days to 17 years), including six girls and 14 boys. Twelve patients underwent clinical work-up and diagnostic imaging for a newly diagnosed mass. The remaining eight patients were on follow-up after surgical resection (follow-up period 2 to 9 years) of confirmed LM and presented with recurrence or progression, or persisting disease after incomplete resection, of previously diagnosed LM. Sixteen of our 20 patients again had ultrasonography prior to MRI at our institution. Tumour location was in the head and neck region (n=11), axillary (n=1), in the abdomen (n=3) and at the lower extremity (n=5).

All routine MRI examinations were completed according to the oncological standard imaging protocol of the respective anatomical region, as implemented at our institution. MRI was performed at 1.5 Tesla (Magnetom Symphony n=13, Magnetom Aera n=6, Magnetom Avanto n=1; Siemens Healthcare, Erlangen, Germany). Eight patients (age range 36 days to 5 years) were sedated for MRI and monitored by a paediatric anaesthesiologist. All scans were acquired in supine position with commercially available standard RF coils of the hardware manufacturer, that is, a dedicated neck coil for all cervical scans and phased-array body coils for scans of the abdomen and the extremities, and with an i.v. line in place. The scan protocol comprised T2-weighted (T2w) imaging, pre-contrast T1-weighted (T1w) and contrast-enhanced T1w sequences. A blood-sensitive T2*w gradient-echo sequence, adapted from a standard neuroimaging sequence, was scanned in four patients. Prior to i.v. contrast administration, DWI was acquired as transverse (axial) single-shot diffusion-weighted echo-planar imaging (SS-DW-EPI). Typical scan parameters were repetition time (TR) 4600 ms, echo time (TE) 137 ms, flip angle 90°, fat saturation, b-values of 50 and 800 s^2/mm, bandwidth 976 Hz/pixel, echo spacing 1.17 ms, epi factor 128, 6 averages, slice thickness 4-6 mm with a scanning time between 2 min 50s and 5 min 30s, depending on the size of the scanning volume. All DWI scans were performed in free-breathing technique.

Image analysis was conducted offline on a standard radiological workstation (Syngo Plaza, Siemens Healthcare, Erlangen, Germany) based on anonymized MRI data sets. In a consensus reading of two experienced observers, the readers were blinded to all patient information, clinical and histopathological data, treatment status and previous imaging studies. The imaging features of each tumour were analysed in terms of morphological and signal characteristics on ultrasonography, on T1w imaging with and without gadolinium contrast, T2w imaging, and T2* imaging, if available. The intensity of the DWI signal was recorded as a qualitative measure (high vs. low in comparison to the anatomical background) by visual assessment on images acquired at low and at high b-values. A board-certified paediatric radiologist with long-standing experience in extracranial diffusion-weighted MRI performed all quantitative analyses. Measurements of the widest diameter was taken in each mass on conventional MR images and compared to the sonographically determined tumour size, as recorded in the radiological examination report. The mean apparent diffusion coefficient (ADC, unit: 10^{-3} mm^2/s) was calculated as the average of three measurements with a single circular region of interest (ROI) of about 1 cm^2 in a representative part of the mass. In lesions exhibiting both hypointense and hyperintense portions, assessment of signal intensity on DW images and ADC measurement were performed in two representative parts of the tumour.

Statistical analysis

Normally distributed data is presented as mean ± standard deviation, data deviating from normal distribution as median [range]. Data exploration and spreadsheet analyses were performed with Microsoft Excel 2007 for Windows.

Results

Patients with newly diagnosed mass

Twelve patients underwent diagnostic work-up for newly discovered tumours. This group included eight LMs (patient ID 1 - 4, 6, 12, 13, 16, Table 1). Of these, four patients presented with acute clinical symptoms of tenderness, pain and swelling and were diagnosed with echogenic masses on initial ultrasonography performed by primary care paediatricians or family physicians, which prompted the preliminary diagnosis of lymphadenopathy, or lymphoma, followed by immediate referral to our institution for further diagnostic workup. The four remaining patients had cystic tumours with little or no intralesional echogenicity. On ultrasonographic evaluation at our department, seven of eight tumours had septation and four tumours were completely or partially echogenic.

Four patients had newly diagnosed masses other than LM. One 13-year-old girl (patient ID 17) presented with a painless cystoid hypoechogenic mass in the submandibular space measuring 60 mm in diameter and exhibiting ultrasonographic imaging features consistent with LM. MRI established the intra-oral origin of the lesion with protrusion through the floor of the mouth into the submandibular region, suggesting a large salivary gland retention cyst, or ranula. Another patient (ID 18), a 17-year old female, was referred with a painless solitary cervical hypoechogenic mass and suspected LM or neurinoma. Ultrasonography at our institution showed intralesional blood flow in doppler/duplex mode, conventional MRI visualised unilateral cervical lymphadenopathy and DWI confirmed very low ADC, indicating high cellularity, in the main lesion, suggestive of lymphoma, which was histologically confirmed as lymphocyte-rich Hodgkin lymphoma. Another patient (ID 19), a 3-year-old boy, with a newly discovered echogenic cervical mass and painful tenderness for several days was referred for suspected lymphoma. Ultrasonographic examination at our department showed a complex lesion with multiple septations, some minor non-echogenic portions and predominately homogeneous intralesional echogenicity, in which wavering movements of echogenic particles could be induced by manual compression. These findings suggesting a haemorrhagic cystoid lesion, such as haemorrhagic LM, were supported by MRI. The patient underwent surgical resection, and immunohistochemical analysis eventually confirmed a haemorrhagic venous malformation. The last patient in this group (ID 20), a 12-year-old boy, presented with increasingly painful cervical swelling and tenderness for three weeks and a solitary 42 mm homogeneously echogenic lateral cervical mass. In

Table 1. Tumour entity, tumour site and signal characteristics on ultrasonography and MRI

ID	tumour entity	tumour site	US	T1w	T2w	T2*w	DWI b=50	DWI b=800	ADC, 10^{-3} mm²/s
1	LM	cerv	↑	↑	↑↓		↑↓	↓↓	0.9 / 2.5
2	LM	abd	↑	↑↓	↑↓	↓↑	↑↓	↓↓	0.9 / 3.1
3	LM	extr	↓	↓	↑		↑	↓	2.9
4	LM	abd	↑	↑	↑↓		↑↓	↓↓	0.6 / 2.5
5	LM	cerv	↓	↓	↑		↑	↓	4.2
6	LM	cerv	↓	↓	↑		↑	↓	3.5
7	LM	cerv			↑		↑	↓	2.7
8	LM	cerv	↓	↓	↑		↑	↓	2.1
9	LM	abd	↓	↓	↑		↑	↓	2.3
10	LM	extr			↑		↑	↓	1.8
11	LM	extr	↓	↓	↑		↑	↓	3.5
12	LM	ax	↑	↑	↑↓	↓↑	↓↑	↓↓	0.8 / 2.6
13	LM	cerv	↓	↓	↑		↑	↓	2.9
14	LM	extr	↓		↑		↑	↓	2.4
15	LM	extr		↓	↑		↑	↓	2.7
16	LM	cerv	↓	↓	↑		↑	↓	2.6
17	Ranula	cerv		↓	↑		↑	↓	2.7
18	Hodgkin	cerv	↑		↑		↔	↑	0.6
19	VM	cerv	↑	↑	↑↓	↓↑	↑↓	↓↓	0.4 / 2.6
20	BrC	cerv	↑	↓	↑	↑	↑	↓	1.8

ADC = apparent diffusion coefficient; DWI = diffusion-weighted imaging; ID = patient number; LM = lymphatic malformation; Hodgkin = Morbus Hodgkin; VM = venous malformation; BrC = branchiogenic cyst; cerv = cervical; abd = abdominal; extr = extremity; US = ultrasonography; ↑ = high signal; ↓ = low signal; ↑↓ = predominately high signal, partially low signal; ↓↑ = predominately low signal, partially high signal, ↓↓ = low signal, partially complete or nearly complete loss of signal, ↔ = intermediate signal

this patient, initial differential diagnosis included haemorrhagic lymphoma and infected branchiogenic cyst, the latter diagnosis eventually confirmed after resection and histological evaluation.

Patients with diagnostic follow-up of previously diagnosed and treated LM

This group included eight patients (3 girls; patient ID 5, 7-11, 14, 15) with a median age of 8 years [2 to 15 years]. Residual LM after preceding surgery was present in 5 patients. Recurrence of LM after surgical resection was seen in 3 patients. Median tumour size was 52 mm [9 to 250 mm). The tumours were located at the neck (n=3), in the abdomen (n=1) and at the lower extremity (n=4). Ultrasonography, available in 5 patients, showed uniformly low intralesional signal without indication of haemorrhage.

Imaging characteristics of histologically confirmed LMs

Of 16 histologically confirmed LMs, 12 lesions (patient ID 3, 5-11, 13-16) showed uniform findings of low signal intensity on T1w, high signal on T2w, high signal on DWI b=50, low signal on DWI b=800 and high mean ADC values (unit: 10^{-3} mm²/s) with an average of 2.8 ± 0.6, ranging from 1.8 to 4.2. With gadolinium contrast, none of the tumours showed any enhancement other than mild signal increase along the peripheral rim and within intralesional septations. None of these patients reported acute clinical symptoms. Correlation with in-house ultrasonography, available in 9 of 12 patients,

Table 2. Lesion characterisation based on DWI signal at low and at high b-value and the corresponding ADC value

	DWI low b-value	DWI high b-value	ADC map
non-restricted diffusion: fluids, cysts tumours with very low cellularity	↑	↓	↑
highly restricted diffusion: tumours with high cellularity, cytotoxic oedema, abscess	↑↓	↑	↓
signal loss: secondary to susceptibility artefacts, e.g. haemosiderin, air, metallic implants	↓	↓	↓
T2 shine-through artefact	↑	↑	↑

ADC = apparent diffusion coefficient; DWI = diffusion-weighted imaging; ↑ = high signal; ↓ = low signal; ↑↓ = low or high signal, depending on T2w signal of the lesion

demonstrated uniformly low-signal echogenicity in all these masses. Eight LMs were septated on both ultrasonography and conventional MRI, while one tumour was seen as a small solitary non-septated cyst with both imaging modalities. No differences in MR imaging characteristics were observed between the four patients with primary diagnosis of LM and the eight patients with follow-up of previously diagnosed LM.

The remaining four LM patients (patient ID 1, 2, 4, 12) consistently showed complex lesions in terms of signal intensity (Fig. 1). While some part of each tumour had MR imaging findings as seen in the typical LMs, the remaining mass exhibited varying degrees of signal alteration with increased signal intensity on pre-contrast T1w imaging, as well as partially decreased signal on T2w, DWI b=50 and DWI b=800. Furthermore, intralesional spots of complete or nearly complete signal loss were observed in these patients on diffusion-weighted images at b=50 and b=800, resulting in mixed low-and-high signal on the corresponding ADC maps. Findings on T2*w imaging available in two of these patients showed corresponding loss of signal, indicating imaging artefacts caused by local magnetic field inhomogeneity, as seen with haemosiderin deposition secondary to haemorrhage. Mean ADC measured in "normal" portions of the tumour was 2.6 ± 0.3, ranging from 2.5 to 3.1, while mean ADC in tumour parts showing signal alterations was measured as 0.8 ± 0.2, ranging from 0.6 to 0.9. In two patients, slightly increased uptake of gadolinium contrast was noticed along the peripheral rim and within the septa of the mass. All four patients presented with acute symptoms and were seen with echogenic tumours on in-house ultrasonography. Three of the four LMs showed septation on ultrasound and on MRI.

Imaging characteristics of tumours mimicking LM

The tumour confirmed as a large submandibular ranula appeared as a large simple cystic lesion on ultrasonography and showed all MRI features of a typical LM with low signal on T1w, high signal on T2w and DWI b=50, low signal on DWI b=800 and high mean ADC = 2.7. The extension of the mass through the floor of the mouth seen on T2w imaging, however, suggested an intra-oral origin, supposedly representing a salivary gland retention cyst, which was confirmed by intra-operative and histological findings.

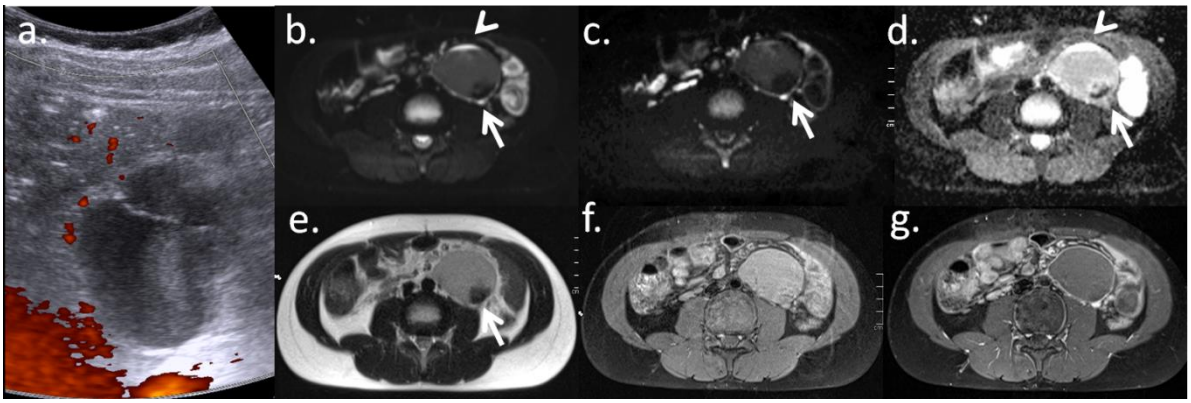

Figure 1. Ultrasonography (a) and MRI (b-g) of the abdomen in a 7-year-old boy (ID 4) with tenderness and pain in the lower left abdomen for 5 days. A hypoechogenic mass with 7.5 cm in diameter was suspected as representing lymphoma at initial ultrasonography. DWI (b=50 (b), b=800 (c), ADC (d)) showed a well-defined heterogenic mass with partial signal loss (arrow) and a small high-intensity fluid level (arrowhead). The lesion was hypointense with partial signal loss (arrow) in T2w (e), hyperintens on T1w pre-Gd (f) and did not show any significant contrast-enhancement (g). The patient underwent resection for suspected haemorrhagic lymphatic malformation, and the diagnosis was confirmed by histological evaluation.

In the patient diagnosed with Hodgkin lymphoma, conventional MRI demonstrated a soft-tissue tumour with low T1w signal, intermediate-to-high T2w signal, and intralesional contrast enhancement. The key finding in this mass was the markedly restricted diffusivity with intermediate-to-high signal on DWI b=50, very high signal on DWI b=800 and homogeneously low mean ADC = 0.6.

The MRI findings in the patient with haemorrhagic venous malformation resembled the imaging characteristics of haemorrhagic LM (Fig. 2). Partial hyperintensity on T1w, partially low signal on T2w, as well as pronounced partial signal loss on T2*w and diffusion-weighted imaging all indicated the presence of haemorrhage. Tumour parts without signs of haemorrhage showed a high mean ADC = 2.6, while very low ADC = 0.4 was measured in low-signal parts of the tumour. Contrast-enhanced T1w imaging did not reveal any significant intralesional gadolinium uptake. Immunohistochemical staining in this vascular lesion was positive for CD31 and CD34, while negative for GLUT1 and D2-40, establishing the diagnosis of venous malformation with signs of haemorrhage.

The cervical mass diagnosed as representing an infected branchiogenic cyst, although strongly and homogeneously echogenic on ultrasonography, showed imaging features suggestive of a non-complicated cystic mass on conventional MRI and on DWI with the exception of a marked peripheral rim enhancement after i.v. contrast application (Fig. 3). Intralesional signal was uniformly high on T2*w imaging.

Tumour size measured on ultrasonography and MRI

The median difference of tumour size measured on conventional MRI, as compared to ultrasonography, was 5 mm at a median tumour size of 49 mm, indicating a deviation of about 10%, with a range of -9 mm (tumour smaller on MRI) to 97 mm (tumour larger on MRI). The highest difference was seen in a patient with follow-up of a large LM stretching subcutaneously from the lower thigh to the knee and the proximal lower leg, measuring 247 mm on MRI, iwhile a maximum extent of only 150 mm was recorded on ultrasonography.

Discussion

Our study is the first to systematically explore DWI imaging features of lymphatic malformations (LM) and lesions mimicking LM in a relatively large case series of paediatric patients. Our results indicate

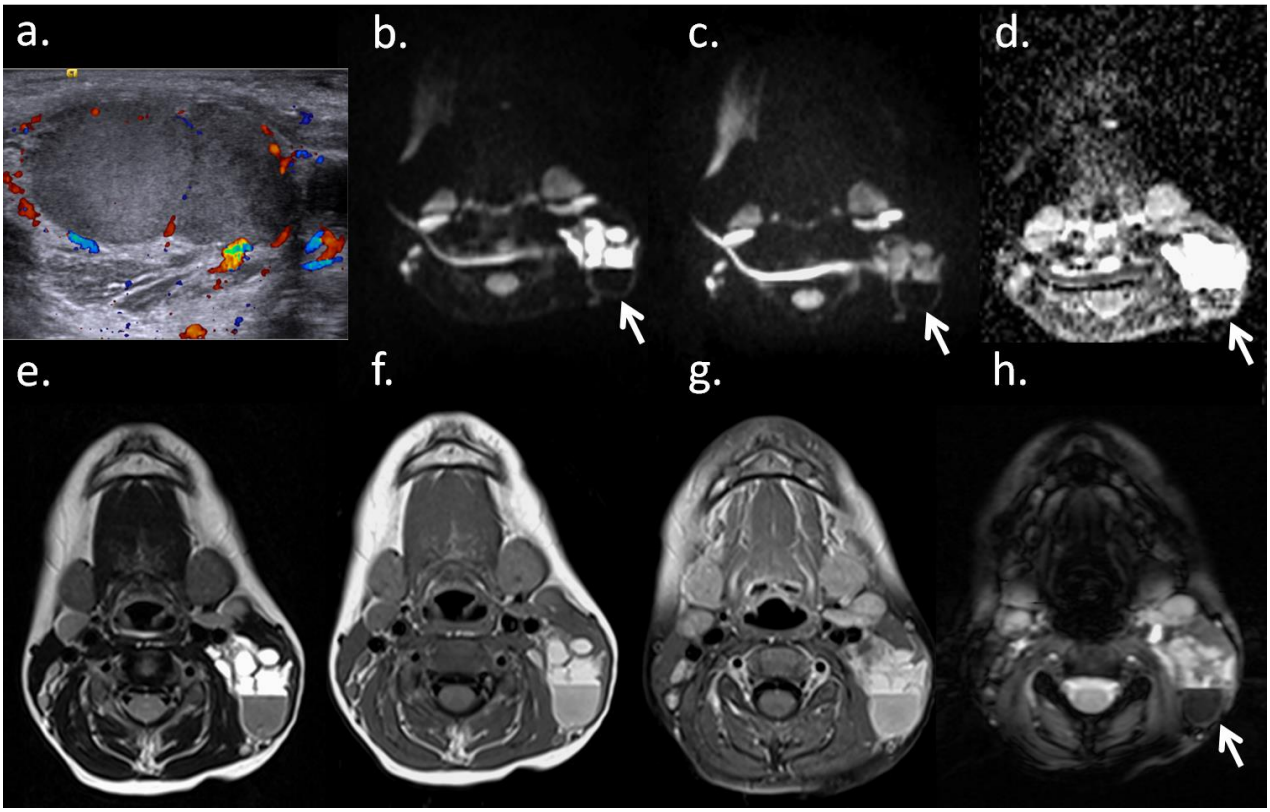

Figure 2. Ultrasonography (a) and MRI (b-h) of the neck in a 3-year-old boy (ID 19) with rapidly growing cervial mass and pain for three weeks. As with the patient in Fig. 1, the patient was referred for suspected lymphoma based on external ultrasonography. The mass appeared predominately hyperechogenic and showed signs of perilesional blood flow on colour-encoded doppler ultrasound (a). MRI revealed a multicystic complex mass with a fluid-fluid level discernable on DWI (b=50 (b), b=800 (c), ADC (d), T2w (e), as well as pre- (f) and post-Gd (g) T1w. The blood-sensitive gradient-echo T2*w sequence (h) shows loss of signal in part of the lesion, as does DWI. In this setting, DWI alone excludes lymphoma or any other cell-rich mass and proves haemorrhage in the suspected cervical lymphatic malformation. The patient underwent resection, and histological evaluation with additional immunohistochemical staining revealed a haemorrhagic venous malformation.

that LMs show distinct imaging characteristics on diffusion-weighted MRI. In contrast to the strongly restricted diffusivity observed in the vast majority of paediatric malignancies [10, 11, 14-18], ADC values in our study were uniformly high in non-complicated LM. Marked artefacts occurred on DW images in the presence of intralesional bleeding and haemorrhage, supposedly due to local magnetic field inhomogeneity caused by haemosiderin deposition, with consecutively low signal on ADC maps, which must not be mistaken for a sign of malignancy. To our knowledge, the utility of signal loss artefacts for diagnostic purposes in single-shot EPI diffusion-weighted MRI of paediatrics tumours has not been reported so far. It remains to be seen whether newly developed, artefact-resistant DWI techniques, such as read-out segmented multi-shot echo-planar DWI, still preserve this particular feature.

In general, imaging of LM and other vascular soft tissue lesions in children is straight forward and can be performed reliably with ultrasonography by an experienced operator [6, 19]. Microcystic or macrocystic morphology, intralesional fluid signal and the absence of intratumoral blood flow all support the diagnosis of non-complicated LM. In such patients, additional MR imaging may be helpful in displaying the full size of large lesions prior to

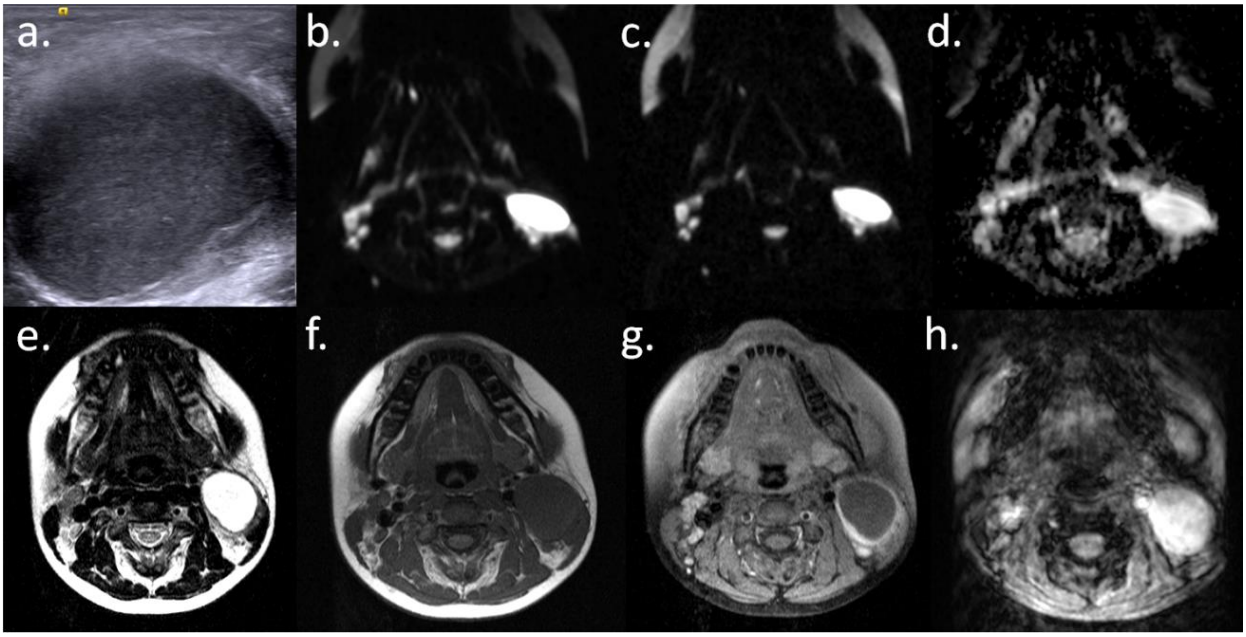

Figure 3. Ultrasonography (a) and MRI (b-h) of the neck in a 12-year-old boy (ID 20) with left cervikal pain and clinically suspected mass for two weeks. The cystic lesion was homogeneously hypoechogenic. Unlike in Fig. 2, intralesional signal characteristics suggest fluid on all MRI sequences (DWI b=50 (b), b=800 (c), ADC (d), T2w (e), T1w pre- (f) and post-Gd (g)) without any signs of partial or complete signal loss. Lesion signal on DWI b=800 remains high, representing T2w "shine-through" artefact, rather than restricted diffusivity, asconfirmed by the high intralesional ADC of 1.8 x 10^{-3} mm^2/s. Blood-sensitive gradient-echo T2*w (h) does not show signs of haemorrhage. There was mild rim enhancement on fat-saturated contrast-enhanced T1w (g). Histological evaluation of the surgical specimen confirmed the diagnosis of an infected branchiogenic cyst.

surgical or interventional treatment, so as not to underestimate the true extent, or mistake the origin, of the tumour, as seen in two patients in our study.

The presence of complex cystic lesions or of mixed vascular tumours [20, 21], however, occasionally poses significant diagnostic difficulties. Young patients in pain may not cooperate with the ultrasonographer, the tumour site may not allow satisfactory ultrasonographic evaluation, or various degrees of signal alterations due to haemorrhagic transformation, infection or vascularised portions of the tumour may hinder accurate and confident ultrasonographic assessment. Of twelve consecutive patients in our study with masses newly discovered on ultrasonography, six patients had acute clinical symptoms including five lesions with haemorrhagic masses and one with acute infection. Of these twelve patients, only eight were confirmed as having LM. Three of the referrals suspected as having lymphoma were eventually diagnosed with haemorrhagic LM. In one patient, suspected LM turned out to be Hodgkin disease. These findings underline a practical demand for second-line imaging with high diagnostic accuracy, such as MRI [22]. The small number of studies available on diffusion-weighted imaging (DWI) in paediatric patients with LM suggest that DWI adds to the diagnostic performance of conventional MRI [11-13, 18]. Probing the diffusivity of water molecules in vivo, the DWI signal is assumed to mainly reflect tissue cellularity and the amount of extracellular space available for diffusion [10]. Nearly free diffusion can be expected in the wide fluid-filled spaces characteristic of LM, represented by high mean ADC values, generally in excess of 1.5 x 10^{-3} mm^2/s, and usually higher than 1.8 x 10^{-3} mm^2/s [11-13, 18]. The median ADC of 2.8 ± 0.6 [range 1.8 to 4.2] in non-complicated LM and the mean ADC of 2.6 ± 0.3 [range 2.5 to 3.1] in non-haemorrhagic portions

of haemorrhagic LM, as observed in our study, support the previously published data. In an earlier study, mean ADC of haemangioma was observed as $1.6 \pm 0.2 \times 10^{-3}$ mm^2/s [11], indicating a somewhat higher cellularity in this vascular tumour entity, possibly with additional effects of microperfusion on the DW signal acquired at low b-values [23]. To limit the influence of microperfusion on our DW imaging, we routinely choose a non-zero low b-value for DWI scans, that is b=50 in this study. Solid soft tissue tumours, and lymphoma in particular, show characteristic high signal on DW imaging at high b-values and corresponding low ADC values [24], as seen in the one lymphoma patient in our study, indicating highly restricted diffusivity. High signal observed on diffusion-weighted images measured at high b-value must always be interpreted in combination with the corresponding ADC value so as to avoid mistaking a T2 shine-through artefact for restricted diffusivity (Figure 3, Table 2). A standard cranial single-shot echo-planar DWI scan is scanned within 41 s at our institution and is also diagnostic in the head-and-neck region. To assure image quality, we acquire more averages in extra-cranial DWI with a total scanning time of about 3 minutes for cervical and about 5 minutes for abdominal scans.

MR imaging features of blood, bleeding and post-haemorrhagic blood degradation are highly complex and are best understood in the context of intracranial haemorrhage and complex renal cysts. Hyperintensity on T1w imaging may represent blood, but also high-protein content. Gradient echo T2*w or susceptibility-weighted (SWI) imaging are specifically designed to trace local magnetic field inhomogeneities secondary to blood degradation products, such as haemosiderin. Single-shot echoplanar diffusion-weighted imaging is also highly susceptible to disturbances in the local magnetic field, frequently resulting in degraded image quality due to distortion and ghosting artefacts. In our study, marked alterations of signal on diffusion-weighted images coincided with signal alterations on T1w, T2w and, where available, on T2*w imaging. These signal alterations were observed as a varying degree of signal loss on DWI measured at low and at high b-values, as well as on the ADC map. Furthermore, loss of signal on DWI also coincided with increased echogenicity on ultrasound. The only exception in this respect was the patient with the infected branchiogenic cyst, who showed strong hyperechogenicity on ultrasonography, but no signal loss on DWI, nor on T2*w imaging. In this patient only, i.v. contrast application contributed substantial additional information to native scans and DWI. Based on these findings, susceptibility imaging with DWI and T2*w may help to differentiate haemorrhagic cysts from infected cystic lesions in patients with an hyperechogenic mass without the need of i.v. contrast application. All five patients with haemorrhagic lesions showed complex signal on DWI with at least a small part of the mass exhibiting "cystic" signal accompanied by fluid-fluid levels separating high-signal from low-signal portions of the tumour, the latter apparently following gravity and being located in the lower/posterior part of the tumour.

Limitations of our explorative study include the retrospective design and the relatively small number of patients available for analysis. In-house ultrasonography was not available in four of the 20 patients. MRI scans were performed at three different 1.5 Tesla scanners of the same manufacturer and with different RF coils, that is either neck coil or body coil, as appropriate, thus introducing some variation into the parameters of the MRI protocols. In an earlier study, we analysed the variation in ADC for reference tissues at 1.5 and at 3 Tesla and found little substantial variation [11]. We hold that for MR scanners of the same manufacturer the variation that arises from different scanner setup is comparably small to the error introduced by manual ROI analysis. The number of masses mimicking LM on initial examination in our study is small and may not be representative of a larger paediatric cohort.

In summary, our findings indicate that DWI is a useful addition to paediatric MRI protocols for differentiation of extra-cranial masses. DWI is fast, relatively insensitive to bulk motion, thus allowing free-breathing scans, and provides a high inherent contrast without the need of i.v. contrast application. An interesting finding from our study is that the high susceptibility of DWI to disturbances in the local magnetic field, usually considered a disadvantage and a source of unwanted artefacts, can actually be employed for diagnostic purposes and may help to trace haemorrhagic transformation of cystic tumours. The extent of the signal alterations induced by intralesional haemorrhage

and the correlation of signal alterations on standard MRI sequences and on DWI need to be validated by further investigation. Recent reports on intracerebral gadolinium deposition after i.v. injection of Gd-based contrast agents have raised concern regarding the long-term safety of these contrast agents [25], especially in children. The combination of native MR sequences plus DWI may, in many patients, characterise vascular lesions and rule out malignancy with sufficient confidence and diagnostic accuracy. Based on our results, DWI may substitute other blood-sensitive scans and thus help to shorten total acquisition time, which is an important factor in paediatric MR imaging.

Conclusions

Our study data demonstrate that non-complicated lymphatic malformations show characteristic signal patterns on diffusion-weighted MRI. Typical signal alterations on DWI were observed in haemorrhagic transformation of LM and in masses mimicking LM on ultrasonography. Therefore, DWI as a fast and non-invasive MRI technique may help in the differential diagnosis of complex cystic masses or in cases of tumours of uncertain dignity.

Acknowledgements

The authors would like to thank the MRI technicians for performing the MR scans in high quality and for taking care of the patients during the examination. No external sources of funding were used in this research.

Abbreviations

ADC, apparent diffusion coefficient;
ce-T1w, contrast-enhanced T1-weighted;
DWI, diffusion-weighted imaging;
ROI, region of interest;
SI, signal intensity;
SS-DW-EPI, single-shot diffusion-weighted echo-planar;
T1w, T1-weighted;
T2w, T2-weighted;
TE, echo time;
TR, repetition time

References

[1] Mulliken JB, Glowacki J. Hemangiomas and vascular malformations in infants and children: a classification based on endothelial characteristics. Plast Reconstr Surg. 1982 Mar;69(3):412-22.
[2] Glasson MJ, Taylor SF. Cervical, cervicomediastinal and intrathoracic lymphangioma. Prog Pediatr Surg. 1991;27:62-83.
[3] Chen CW, Hsu SD, Lin CH, Cheng MF, Yu JC. Cystic lymphangioma of the jejunal mesentery in an adult: a case report. World J Gastroenterol. 2005 Aug 28; 11(32):5084-6.
[4] Campbell WJ, Irwin ST, Biggart JD. Benign lymphangioma of the jejunal mesentery: an unusual cause of small bowel obstruction. Gut. 1991 Dec;32(12): 1568.
[5] Poldervaart MT, Breugem CC, Speleman L, Pasmans S. Treatment of lymphatic malformations with OK-432 (Picibanil): review of the literature. J Craniofac Surg. 2009 Jul;20 (4):1159-62. doi: 10.1097/SCS.0b013e3181abb249.
[6] McHoney M. Early human development: Neonatal tumours: Vascular tumours. Early Hum Dev. 2010 Oct;86(10): 613-8. doi: 10.1016/j.earlhumdev.2010.08.017.
[7] Nakano T, Hara Y, Shirokawa M, Shioiri S, Goto H, Yasuno M, et al. Hemorrhagic giant cystic lymphangioma of the liver in an adult female. J Surg Case Rep. 2015 Apr 1;2015(4).pii:rjv033. doi: 10.1093/jscr/rjv033.
[8] Tseng JJ, Chou MM, Ho ES. Fetal axillary hemangiolymphangioma with secondary intralesional bleeding: serial ultrasound findings. Ultrasound Obstet Gynecol. 2002 Apr;19(4):403-6.
[9] Ros PR, Olmsted WW, Moser RP Jr, Dachman AH, Hjermstad BH, Sobin LH. Mesenteric and omental cysts: histologic classification with imaging correlation. Radiology. 1987 Aug;164(2):327-32.
[10] Humphries PD, Sebire NJ, Siegel MJ, Olsen OE. Tumors in Pediatric Patients at Diffusion-weighted MR Imaging: Apparent Diffusion Coefficient and Tumor Cellularity. Radiology. 2007 Dec;245(3):848-54.

[11] Neubauer H, Evangelista L, Hassold N, Winkler B, Schlegel PG, Köstler H, et al. Musculoskeletal tumorous and tumour-like lesions: diagnostic utility of diffusion-weighted MRI for detection and differentiation in paediatric patients. World J Pediatr. 2012 Nov;8(4):342-9. doi: 10.1007/s12519-012-0379-8.
[12] Lope LA, Hutcheson KA, Khademian ZP. Magnetic resonance imaging in the analysis of pediatric orbital tumors, and the utility of diffusion-weighted imaging. J AAPOS. 2010 Jun;14(3):257-62. doi: 10.1016/j.jaapos.2010.01.014.
[13] Humphries PD, Wynne CS, Sebire NJ, Olsen OE. Atypical abdominal paediatric lymphangiomatosis: diagnosis aided by diffusion-weighted MRI. Pediatr Radiol. 2006 Aug;36(8):857-9.
[14] Gawande RS, Gonzalez G, Messing S, Khurana A, Daldrup-Link HE. Role of diffusion-weighted imaging in differentiating benign and malignant pediatric abdominal tumors. Pediatr Radiol. 2013 Jul;43(7):836-45. doi: 10.1007/s00247-013-2626-0.
[15] Gahr N, Darge K, Hahn G, Kreher BW, von Buiren M, Uhl M. Diffusion-weighted MRI for differentiation of neuroblastoma and ganglioneuroblastoma/ganglioneuroma. Eur J Radiol. 2011 Sep; 79(3):443-6. doi: 10.1016/j.ejrad.2010.04.005.
[16] Hassold N, Warmuth-Metz M, Winkler B, Kreissl MC, Ernestus K, Beer M, et al. Hit the mark with diffusion-weighted imaging: metastases of rhabdomyosarcoma to the extraocular eye muscles. BMC Pediatr. 2014 Feb 27;14:57. doi: 10.1186/1471-2431-14-57.
[17] Alibek S, Cavallaro A, Aplas A, Uder M, Staatz G. Diffusion weighted imaging of pediatric and adolescent malignancies with regard to detection and delineation: initial experience. Acad Radiol. 2009 Jul;16(7):866-71. doi: 10.1016/j.acra.2009.01.004.
[18] Abdel Razek AA, Gaballa G, Elhawarey G, Megahed AS, Hafez M, Nada N. Characterization of pediatric head and neck masses with diffusion-weighted MR imaging. Eur Radiol. 2009 Jan;19(1):201-8. doi: 10.1007/s00330-008-1123-6.
[19] Hinds DF, Aponte EM, Secko M, Mehta N. Identification of a pediatric intra-abdominal cystic lymphangioma using point-of-care ultrasonography. Pediatr Emerg Care. 2015 Jan;31(1):62-4. doi: 10.1097/PEC.0000000000000334.
[20] Mahady K, Thust S, Berkeley R, Stuart S, Barnacle A, Robertson F, et al. Vascular anomalies of the head and neck in children. Quant Imaging Med Surg. 2015;5(6):886-897. doi: 10.3978/j.issn.2223-4292.2015.04.06.
[21] Mulligan PR, Prajapati HJ, Martin LG, Patel TH. Vascular anomalies: classification, imaging characteristics and implications for interventional radiology treatment approaches. Br J Radiol. 2014 Mar;87(1035):20130392. doi: 10.1259/bjr.20130392.
[22] Vilanova JC, Barcelo J, Smirniotopoulos JG, Perez-Andres R, Villalon M, Miro J, et al. Hemangioma from head to toe: MR imaging with pathologic correlation. Radiographics 2004;24:367-85.
[23] Le Bihan D, Breton E, Lallemand D, Aubin M-L, Vignaud J, Laval-Jeantet M. Separation of Diffusion and Perfusion in Intravoxel Incoherent Motion Mr Imaging. Radiology. 1988 Aug;168(2):497-505.
[24] Kwee TC, Takahara T, Vermoolen MA, Bierings MB, Mali WP, Nievelstein RA. Whole-body diffusion-weighted imaging for staging malignant lymphoma in children. Pediatr Radiol. 2010 Oct;40(10):1592-1602. doi: 10.1007/s00247-010-1775-7.
[25] McDonald RJ, McDonald JS, Kallmes DF, Jentoft ME, Murray DL, Thielen KR, et al. Intracranial gadolinium deposition after contrast-enhanced MR imaging. Radiology. 2015 Jun;275(3):772–82. doi: 10.1148/radiol.15150025.